Commun. Fac. Sci. Univ. Ank. Series A2-A3
V. 44. pp. 17-33 (1997)

MIXING PROPERTIES OF A VISCOELASTIC FLUID
Part II: In a Closed Cylindrical Cavity Flow

Hüseyin DEMİR

Department of Mathematics, Ondokuz Mayıs University, Faculty of Education, Atakum/Samsun, TURKEY.

(Received Oct. 6, 1997; Accepted Dec. 31, 1997)

ABSTRACT

The laminar flow of Newtonian and non-Newtonian fluids with constant and variable shear-rate parameters are studied theoretically. Numerical solutions for the concentration, particle path are obtained using finite differences and A.D.I. method in 3D cylindrical cavity. Mixing properties are investigated by tracking the motion of a number of selected fluid particles and by simulating the dispersive mixing of a 'coloured' fluid injected into the cavity while at rest in both cylinder and concentric cylinder driven flow. The stability of consentration intensity is investigated for a wide range of Newtonian and non-Newtonian fluids. The effects of inertia and elasticity are of particular interest. The instabilities are characterised by control parameters: the Reynolds, Weisenberg and Schmidt numbers.

1. INTRODUCTION

This paper is aimed to make a contribution to the study of the mixing of viscoelastic fluids at Re=1, Re=10 and Re=100. Such mixing of viscoelastic fluids is a commonly used but is not well understood in the industrial processing of the fluids due to difficulties that occur with computing the velocity field [1] and these difficulties make the analysis of mixing flow very complicated. Considered in both Newtonian and non-Newtonian fluids for the concentration results and the dispersive mixing generated by the flow patterns of the cylinder cavity flows in two cases namely cylinder and concentric cylinder driven flow. It is assumed that the dye initially occupies the half of the cavity and there is no chemical reaction in the concentration flow equation. Results for fluid particle speed and concentration results are obtained by numerical simulation.

2. THEORY

Considered in an incompressible viscoelastic CEF fluid in a closed cylinder cavity with the density of fluid taken as constant. Furthermore it is assumed that the flow is axisymetric for simplicity there is no dependence of flow on the rotational θ direction. The main features of the cylindirical flow driven by walls rotating with constant angular velocity are the primary flow in the direction of rotation, and the secondary flow perpendicular to the primary flow. The velocity vector $V_i = (u, r\Omega, w)$ where $\Omega = \frac{v}{r}$. The flow equation can be non-dimensionalised by using the same ideas as in part [2]. The same viscosity function model and fluid model as in part 1 are used in part 2 as well. In this paper numerical solutions for two categories cylindirical driven cavity flow namely

1. Cylindirical Cavity Driven Flow,

2. Concentric Cylindrical Cavity Driven Flow

are presented.

The governing equations of the motion of unsteady incompressible flow of a CEF fluid with shear-rate dependent viscosity can be written as:

$$\frac{\partial \omega}{\partial t} = \frac{1}{r^2 Re} H\left(r^3, \eta; \frac{\omega}{r}\right) + F_\omega \tag{4}$$

$$-\omega = \frac{\partial}{\partial z}\left(\frac{1}{r}\frac{\partial \psi}{\partial z}\right) + \frac{\partial}{\partial r}\left(\frac{1}{r}\frac{\partial \psi}{\partial z}\right), \tag{5}$$

where

$$H\left(r^3, \eta; \frac{\omega}{r}\right) = \left\{\frac{\partial}{\partial r}\left[r^3\frac{\partial}{\partial r}\left(\eta \frac{\omega}{r}\right)\right] + \frac{\partial}{\partial z}\left[r^3\frac{\partial}{\partial z}\left(\eta \frac{\omega}{r}\right)\right]\right\} \tag{6}$$

and

$$F_\omega = \frac{1}{Re}\left\{F_{\Omega l} + F_{\omega\eta} + F_{\omega\Omega} + F_{\omega S}\right\} \tag{7}$$

$$F_{\omega l} = -Re\left\{\frac{\partial}{\partial r}[u\omega] + \frac{\partial}{\partial z}[w\omega]\right\}, \tag{8}$$

$$F_{\omega\eta} = 2\left\{\frac{\partial^2 \eta}{\partial z^2}\frac{\partial w}{\partial r} - \frac{\partial^2 \eta}{\partial r^2}\frac{\partial u}{\partial z}\right\} + \left\{\frac{\partial u}{\partial r} - \frac{\partial w}{\partial z}\right\} M(\eta) \tag{9}$$

$$F_{\omega\Omega} = \frac{1}{r} \mathrm{Re} \frac{\partial}{\partial z} \left(r^2 \Omega^2\right) \tag{10}$$

$$F_{\omega S} = \frac{1}{2} M\left(S_{rr} - S_{zz}\right) + L\left(S_{rz}\right) + \frac{1}{r} \frac{\partial}{\partial z} \left(S_{rr} - S_{\theta\theta}\right) - \frac{1}{r} \frac{\partial}{\partial r} \left(S_{rz}\right) + \frac{1}{r^2} S_{rz} \tag{11}$$

where $\mathrm{Re} = \rho\Omega R^2/\eta(0)$ and R is the outher radius of the cylinder container considered.

The rotational speed equation becomes

$$\frac{\partial \Omega}{\partial t} = \frac{1}{r^3 \mathrm{Re}} H_2\left(r^3, \eta; \Omega\right) + \frac{1}{r^3} F_\Omega \tag{12}$$

where

$$H_2\left(r^3, \eta; \Omega\right) = \frac{\partial}{\partial r}\left[r^3\eta \frac{\partial \Omega}{\partial r}\right] + \frac{\partial}{\partial z}\left[r^3\eta \frac{\partial \Omega}{\partial z}\right] \tag{13}$$

and

$$F_\Omega = \frac{1}{\mathrm{Re}} \left\{F_{\Omega S} + F_{\Omega I}\right\} \tag{14}$$

$$F_{\Omega I} = - \mathrm{Re} \left\{\frac{\partial}{\partial r}\left[r^2 u\Omega\right] + \frac{\partial}{\partial z}\left[r^2 w\Omega\right]\right\} \tag{15}$$

$$F_{\Omega S} = \frac{\partial}{\partial r}\left(r^2 S_{r\theta}\right) + \frac{\partial}{\partial z}\left(r^2 S_{z\theta}\right) . \tag{16}$$

And also the concentration equation is written as

$$\frac{\partial C}{\partial t} = \frac{1}{\mathrm{ReSc}} \nabla^2 C + \frac{1}{r} F_C \tag{17}$$

where

$$F_C = - \left\{\frac{\partial}{\partial r}\left[r\, u\, C\right] + \frac{\partial}{\partial C}\left[r\, w\, C\right]\right\} . \tag{18}$$

Equations (4) - (5) and (17) will be solved by using the same approach as in part 1 and suitable boundary conditions and initial values. the velocity components may be taken as $u = 0$, $w = 0$ on the boundaries. The rotational speed in the cavity is taken as $\Omega = \frac{v}{r}$. The stream function remains constant and is taken as zero on the boundaries. The boundary condition on each type of cylinder cavity geometry is given by considering the vorticity-stream function boundary formulation as follows:

In this case the dye is similarly 'injected' into the flow domain while the fluid is at rest but its quantity is measured as 4 and 16/3 respectively as shown in figure 1. For the concentration equation we employ the homogenous Neumann type boundary for boundaries. We therefore use the gradient at every point of boundary which is $\frac{\partial C}{\partial n} = 0$, where $\underline{n}$ is outward normal.

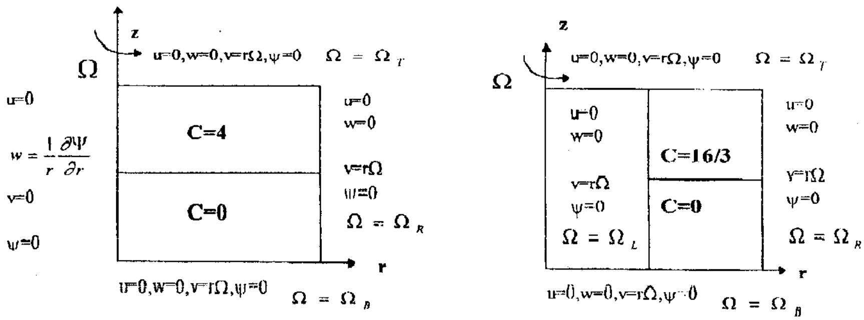

Figure 1: Boundary conditions for cylinder and concentric cylinder driven cavity flow

The other consideration for the concentration equation is the initial condition. The ordinary differential equations of particle paths are given in the following system with respect to Cylindrical co-ordinate system (r,θ,z)

$$\frac{d}{dt}\underline{x}_i(t) = V_i(\underline{x}_i(t)) \tag{19}$$

where $i = 1,2$, $x_1 = r$ and $x_2 = z$. The variable V_i represents the velocity components in the r and z directions respectively. The above system is considered with initial conditions $r(0) = r_0$ and $z(0) = z_0$. The velocity fields is obtained numerically as explained in part 1 [2] by considering the velocity components in terms of a stream function in the r and z directions, so that $u = -\frac{1}{r}\frac{\partial\psi}{\partial z}$ and $v = \frac{1}{r}\frac{\partial\psi}{\partial r}$. The solution is obtained to $O(\Delta t^2, h^2, k^2)$ in the A.D.I. method. The pertinent equations are

$$\underline{x}_{i+1} = \underline{x}_i + \frac{\Delta t}{2}\left[V^0(\underline{x}_i) + V^N(\underline{y}_i)\right] \tag{20}$$

where $\underline{y}_i = \underline{x}_i + \Delta t V^0(\underline{x}_i)$. Then the Modified-Euler method [3] is used as in part 1.

3. THE FINITE DIFFERENCE METHOD

To solve the equations (4), (5) and (17) numerically by finite differences for the time-dependent incompressible flow, Peaceman-Rachford approximation method is used. The stream-vorticity equation can be expressed as in form (21)

$$B_1\psi_{i,j} = B_2\psi_{i+1,j} + B_3\psi_{i-1,j} + B_4\psi_{i,j+1} + B_5\psi_{i,j-1} + B_6 \tag{21}$$

and discretised then the coefficents of the equation now become

$$B_1 = \alpha^2\left(\frac{1}{r^p + 0.5h} + \frac{1}{r^p - 0.5h}\right) + \frac{2}{r^p},$$

$$B_2 = \alpha^2\left(\frac{1}{r^p + 0.5h}\right),\ B_3 = \alpha^2\left(\frac{1}{r^p - 0.5h}\right)$$

$$B_4 = B_5 = \frac{1}{r^p},\ B_6 = k^2 r^p \zeta^p$$

where the vorticity is defined as $\omega = r\zeta$, and from now on this formulation will be used for the vorticity equation. On using the A.D.I. [5,6] method to solve the time-dependent equations by using standart central differences with $rr = \frac{\Delta t}{h^2}$ and $s = \frac{\Delta t}{k^2}$ as

$$\left(1 - \frac{rr}{2} L_x^h\right)\Phi^* = \left(1 + \frac{s}{2} L_y^k\right)\Phi^n + \frac{\Delta t}{2} f_n, \tag{22}$$

$$\left(1 - \frac{s}{2} L_y^k\right)\Phi^{n+1} = \left(1 - \frac{rr}{2} L_x^h\right)\Phi^* + \frac{\Delta t}{2} f_n. \tag{23}$$

For the A.D.I. method when we put ζ in equations (22) and (23) as a dependent variable the vorticity equation can be discretised as

$$\zeta^*_{i,j} - rr\left(A_1\zeta^*_{i+1,j} + A_2\zeta^*_{i-1,j} - 2A_3\zeta^*_{i,j}\right) + rr\frac{h}{2r}(ur)\left(\zeta^*_{i+1,j} - \zeta^*_{i-1,j}\right)$$
$$= \zeta^n_{i,j} + s\left(A_4\zeta^n_{i+1,j} + A_5\zeta^n_{i-1,j} - 2A_6\zeta^n_{i,j}\right) - s\frac{k}{2}w\left(\zeta^n_{i,j+1} - \zeta^n_{i,j-1}\right) + \frac{\Delta t}{2} f^n \tag{24}$$

and

$$\zeta^{n+1}_{i,j} - s\left(A_4\zeta^{n+1}_{i+1,j} + A_5\zeta^{n+1}_{i-1,j} - 2A_6\zeta^{n+1}_{i,j}\right) + s\frac{k}{2}w\left(\zeta^{n+1}_{i,j+1} - \zeta^{n+1}_{i,j-1}\right)$$
$$= \zeta^*_{i,j} + rr\left(A_1\zeta^*_{i+1,j} + A_2\zeta^*_{i-1,j} - 2A_3\zeta^*_{i,j}\right) - rr\frac{h}{2r}(ur)\left(\zeta^*_{i+1,j} - \zeta^*_{i-1,j}\right) + \frac{\Delta t}{2} f^n, \tag{25}$$

where

$$A_1 = \left\{\frac{\left(r^P + 0.5h\right)^3 \left(\eta^E + \eta^P\right)^2}{8 \text{ Re } r^{3P}\eta^P}\right\},$$

$$A_2 = \left\{\frac{\left(r^P - 0.5h\right)^3 \left(\eta^W + \eta^P\right)^2}{8 \text{ Re } r^{3P}\eta^P}\right\},$$

$$A_3 = \left\{\left(\frac{\left(r^P + 0.5h\right)^3 \left(\eta^E + \eta^P\right)^2 + \left(r^P - 0.5h\right)^3 \left(\eta^W + \eta^P\right)^2}{8 \text{ Re } r^{3P}\eta^P}\right) - \left(\frac{\left(r^P + 0.5h\right)^3 \left(\eta^E - \eta^P\right)^2 - \left(r^P - 0.5h\right)^3 \left(\eta^P - \eta^W\right)^2}{2 \text{ Re } r^{3P}}\right)\right\},$$

$$A_4 = \left\{\frac{\left(\eta^N + \eta^P\right)^2}{8 \text{ Re } \eta^P}\right\},$$

$$A_5 = \left(\frac{\left(\eta^N + \eta^P\right)^2 + \left(\eta^S + \eta^P\right)^2}{8 \text{ Re } \eta^P} + \frac{\left(\eta^N - \eta^P\right)^2 - \left(\eta^P - \eta^S\right)^2}{2 \text{ Re}}\right),$$

$$A_6 = \left\{\frac{\left(\eta^S + \eta^P\right)^2}{8 \text{ Re } \eta^P}\right\}.$$

For cylinder driven cavity flow the A.D.I. solution process is similar to the 2D cavity driven flow [2] and the stability condition of the (M-1) (N-1) equations can be determined as previously. This solution process is stable when

$$-\frac{\left(r^3\eta^2\right)_{i-1,j}}{hr^2_{i,j}\eta_{i,j}} \le \frac{(ru)}{2} \le \frac{\left(r^3\eta^2\right)_{i+1,j}}{hr^2_{i,j}\eta_{i,j}}, \text{ and, } \frac{\left(\eta^2\right)_{i,j-1}}{k\eta_{i,j}} \le \frac{w}{2} \le \frac{\left(\eta^2\right)_{i,j+1}}{k\eta_{i,j}}.$$

Similarly, considered in Ω as a dependent function in the equation (22) and (23) we have

$$\Omega^*_{i,j} - rr\left(A_1\Omega^*_{i+1,j} + A_2\Omega^*_{i-1,j} - 2A_3\Omega^*_{i,j}\right) + rr\frac{h}{2r^{3P}}(ur^3)\left(\Omega^*_{i+1,j} - \Omega^*_{i-1,j}\right)$$

$$= \Omega^n_{i,j} + s\left(A_4\Omega^n_{i+1,j} + A_5\Omega^n_{i-1,j} - 2A_6\Omega^n_{i,j}\right) - s\frac{k}{2}w\left(\Omega^n_{i,j+1} - \Omega^n_{i,j-1}\right) + \frac{\Delta t}{2}f^n \qquad (26)$$

and

$$\Omega_{i,j}^{n+1} - s\left(A_4\Omega_{i+1,j}^{n+1} + A_5\Omega_{i-1,j}^{n+1} - 2A_6\Omega_{i,j}^{n+1}\right) - s\,\frac{k}{2}\,w\left(\Omega_{i,j+1}^{n+1} - \Omega_{i,j-1}^{n+1}\right)$$
$$= \Omega_{i,j}^{*} + rr\left(A_1\Omega_{i+1,j}^{*} + A_2\Omega_{i-1,j}^{*} - 2A_3\Omega_{i,j}^{*}\right) - rr\,\frac{h}{2r^{3P}}\,(ur^3)\left(\Omega_{i+1,j}^{*} - \Omega_{i-1,j}^{*}\right) + \frac{\Delta t}{2}\,f^n , \qquad (27)$$

with

$$A_1 = \frac{\left(r^P + 0.5h\right)^3\left(\eta^E + \eta^P\right)}{4\,\mathrm{Re}\,r^{3P}}$$

$$A_2 = \frac{\left(r^P - 0.5h\right)^3\left(\eta^W + \eta^P\right)}{4\,\mathrm{Re}\,r^{3P}}$$

$$A_3 = \frac{\left(r^P + 0.5h\right)^3\left(\eta^E + \eta^P\right)}{4\,\mathrm{Re}\,r^{3P}} + \frac{\left(r^P - 0.5h\right)^3\left(\eta^W + \eta^P\right)}{4\,\mathrm{Re}\,r^{3P}}$$

$$A_4 = \left(\frac{\eta^N + \eta^P}{4\,\mathrm{Re}}\right),\quad A_5 = \left(\frac{\eta^S + \eta^P}{4\,\mathrm{Re}}\right),\ \text{and}\quad A_6 = \left(\frac{\eta^N + \eta^S + 2\eta^P}{4\,\mathrm{Re}}\right).$$

For the concentration equation we have

$$C_{i,j}^{*} - rr\left(A_1C_{i+1,j}^{*} + A_2C_{i-1,j}^{*} - 2A_3C_{i,j}^{*}\right) + rr\,\frac{h}{2r^P}\,(ur)\left(C_{i+1,j}^{*} - C_{i-1,j}^{*}\right)$$
$$= C_{i,j}^{n} + s\left(A_1\Omega_{i+1,j}^{n} + A_2\Omega_{i-1,j}^{n} - 2A_3\Omega_{i,j}^{n}\right) - s\,\frac{k}{2}\,w\left(C_{i,j+1}^{n} - C_{i,j-1}^{n}\right) + \frac{\Delta t}{2}\,f^n \qquad (28)$$

and

$$C_{i,j}^{n+1} - s\left(A_4C_{i+1,j}^{n+1} + A_5C_{i-1,j}^{n+1} - 2A_6C_{i,j}^{n+1}\right) + s\,\frac{k}{2}\,w\left(C_{i,j+1}^{n+1} - C_{i,j-1}^{n+1}\right)$$
$$= C_{i,j}^{*} + rr\left(A_1C_{i+1,j}^{*} + A_2C_{i-1,j}^{*} - 2A_3C_{i,j}^{*}\right) - rr\,\frac{h}{2r^P}\,(ur)\left(C_{i+1,j}^{*} - C_{i-1,j}^{*}\right) + \frac{\Delta t}{2}\,f^n , \qquad (29)$$

where

$$A_1 = \frac{\left(r^P + 0.5h\right)}{\mathrm{ReSc}r^P},\quad A_2 = \frac{\left(r^P - 0.5h\right)}{\mathrm{ReSc}r^P},\ \text{and}\ A_3 = \frac{\left(r^P + 0.5h\right) + \left(r^P + 0.5h\right)}{\mathrm{ReSc}r^P}$$

$$A_4 = \frac{1}{\mathrm{ReSc}} = A_{C5}\ ,\ \text{and}\ A_6 = \frac{2}{\mathrm{ReSc}}\ .$$

The stability conditions for the rotational speed and concentration equations are calculated as before and obtined respectively

$$-\frac{\left(r^3\eta\right)_{i-1,j}}{h} \le \frac{\left(r^3u\right)}{2} \le \frac{\left(r^3\eta\right)_{i+1,j}}{h}\ \text{in equation (26), and}\ \frac{\left(\eta\right)_{i,j-1}}{k} \le \frac{w}{2} \le \frac{\left(\eta\right)_{i,j+1}}{k}$$

in equation (27). Also, it is required that $\frac{h(ru)ReSc}{\left(r^{P} + 0.5h\right)} \leq 2$ in equation (28), and (kw) ReSc ≤ 2 in equation (29).

However, the method yields a pair of implicit equations. The solution of each equation is obtained through the Gaussian Elimination direct type method which is well explained in Smith [7].

4. RESULTS

Time-dependent flow equations are solved by using Peaceman-Rachford method for the dispersive mixing generated by the cylindrical cavity flow. Moreover, flow motion is generated by rotation of the walls. First consideration is given to the convergence of the solution by comparing calculations for various grid widths denoted by h. Results have been evaluated near the top wall for the vorticity and it is evident that convergence to 4 decimal places has been achieved at Re=10 as h decreases. In this case both Newtonian and Boger fluid take the same convergence values as shown in figure 2. Then our problems are solved computationally in two categories as follows

i. Cylindrical Driven Cavity Flow,
ii. Concentric Cylinder Driven Cavity Flow.

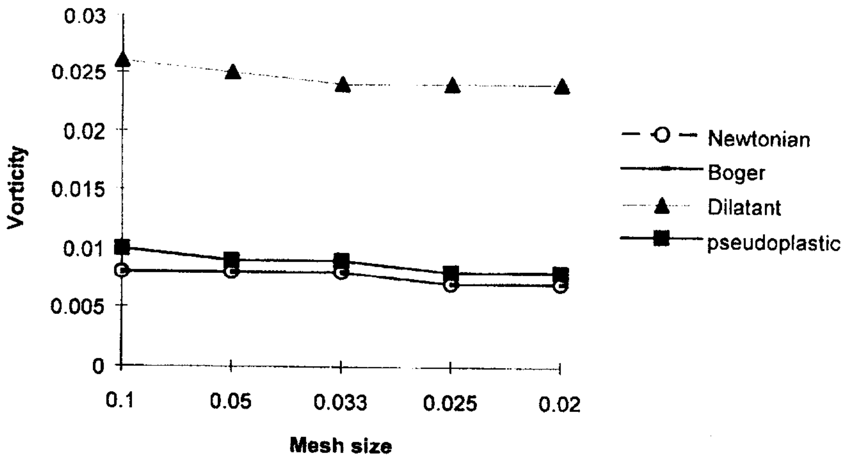

Figure 2: Convergence criterion for vorticity at Re=10 for time-dependent fluid flow

It is assumed that the dye initially occupies in the top half of the cavity region, and there is no chemical reaction for the dispersive mixing problem of cylinder driven cavity flow. The concentration equation is solved numerically in the cylinder configuration. We have three main parameters which are Reynolds number Re, Schmidt number Sc and Weisenberg number Wi.

4.1. Cylindrical Driven Cavity Flow

Considered in the concentration contours as generated in two cases such as two walls rotating in the same direction and in opposite directions, respectively. Here initially the dye is injected into the cavity region while the fluid is rest and its quantity is measured as 4 due to the average value throughout the geometry is being set as 1. With Re=1 we have a linear distribution of the concentration intensity and this behaviour is seen in all types of fluid cases as shown in figure 3. When the Reynolds number increases the advection force begins to dominate the flow so that the colour band is spread out quickly as seen in figure 4 at Re=10. Therefore, as Re increases the advection term firmly dominates the flow and the colour band spreads out between streamlines in the centre region and there is small circulation nearer the left wall shown in figure 5.

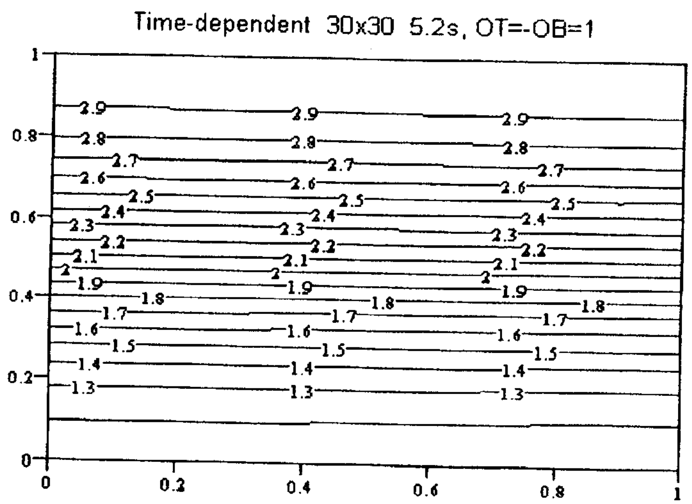

Figure 3: Concentration contours for Newtonian fluid at Re=1, Sc=50

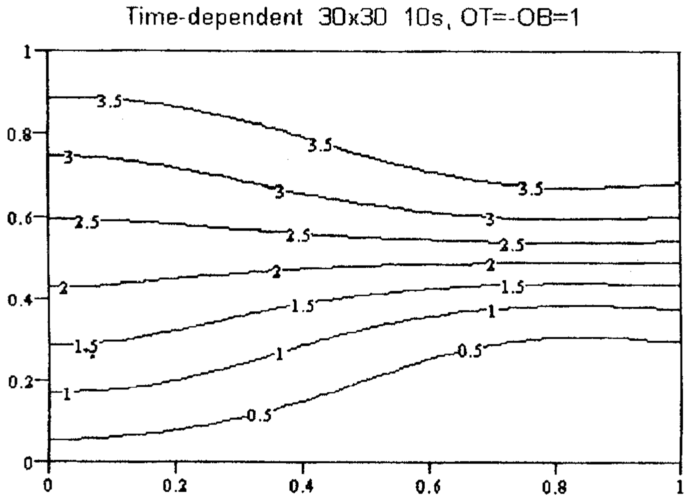

Figure 4: Concentration contours for viscoelastic dilatant fluid at Re=10, Sc=50

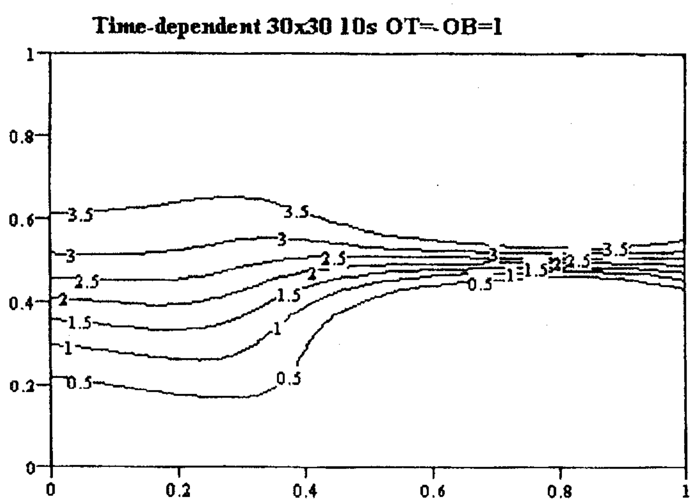

Figure 5: Concentration contours for viscoelastic pseudoplastic fluid at Re=100, Sc=50

In case of two walls rotating in the same direction with constant angular velocity, all results show similar behaviour as in the two walls rotating in the opposite directions.

4.2. Concentric Cylinder Driven Cavity Flow

In this case the concentration problem is undertaken as two walls rotating in the same direction and also in opposite directions respectively. The dye is similarly 'injected' into the flow domain while the fluid is at rest but in this case its quantity is measured as 16/3 because the average value throughout the geometry set as 1. As the two walls rotate in the same direction we have a linear distribution of the concentration intensity throughout the flow region. Similarly as the Re number increases the advection term dominates the flow and at Re=100 the colour is highly dispersed in the centre region and usually follows the flow. Moreover, the concentration intensity is spread out slightly more due to there is small diffusion, where the circulation is weaker. In the case of the non-Newtonian fluid the concentration intensity spreads out more quickly near the left wall as shown in figure 6 and 7 at Re=100 and 100.

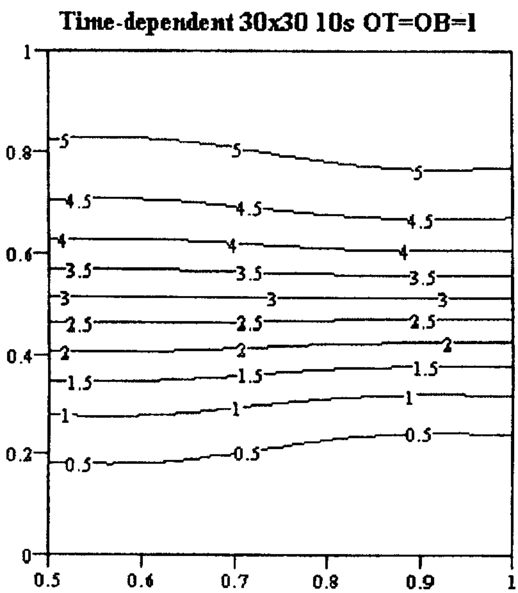

Figure 6: Concentration contours for viscous pseudoplastic fluid at Re=10, Sc=50

In the case of the two walls rotating in opposite direction, there is a linear distribution in the fluid domain at Re=1 in both viscous and viscoelastic cases since there is small secondary flow. A similar distribution is observed at Re=10 and 100 as in the two walls rotating in the same direction.

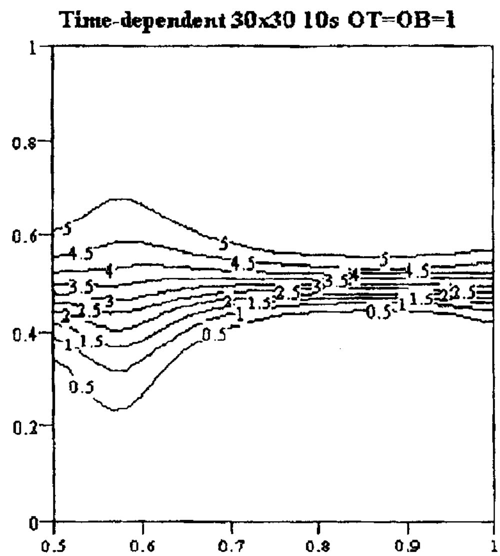

Figure 7: Concentration contours for viscous pseudoplastic fluid at Re=100, Sc=50

5. PARTICLE PATHS AND DISCONTINUOUS PERIODIC 3D CAVITY FLOW

In this section particle paths are investigated by using a discontinuous periodic motion as the top and bottom walls of the cylinder rotate with a periodic motion as shown in figure 8. Although this motion is related to a mixing process, we only deal with particle paths of the fluid and omit an analysis of chaotic motion. Furthermore, considered in the fluid motion in two different cases; at first the flow motion is generated in a whole cylinder secondly it is generated in a concentric cylinder. The solution of the flow then depends on either the period of the motion (T) and on the Reynolds number Re. At first the top wall moves to the right for a period of **T.** Then it stops and the bottom wall starts moving in the opposite direction for a duration of **T.** The cycle is repeated until the desired number of times. The flow is simulated for a duration of 100 seconds for periods T=2. Furthermore, there were three particles initially located in the cavity's vertical middle line r = 0.5. Results are presented for fluid particle paths in (r, z) cylindrical co-ordinate system of cylinder cavity.

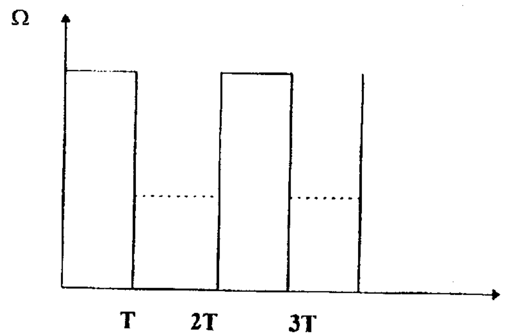

Figure 8: The diagram of the Periodic motion

5.1. The Particle Paths of the Cylinder Driven Cavity Flow

In both viscous and viscoelastic fluid are examined at Re=10 and Re=100 respectively. For Re=10 the results is shown in figure 9, this can be described as the trace paths of three particles. The outer particle (top figure) paths travel a wider orbit in the cavity. However, all three particle paths become 'flatter' near the top wall of the cavity. This behavior is shown in figure 9 at Re=10 for Newtonian fluid. The middle and lower figures show the traces obtained for the periodic motion of the particles by considering the r and z positions with time. As Re increases, for example Re=100, it is found all three particles move faster and travel more widely due to advection force dominating flow. Therefore all three particle paths become more 'tightly bound' together in the flow.

5.2. The Particle Paths of the Concentric Cylinder Driven Cavity Flow

In this case, initially the particles are being placed in the mid-cavity vertical line equally spaced (r = 0.75). Figure 10 shows the trace paths of three particles at Re=10. The outher particle (top figure) is placed initially

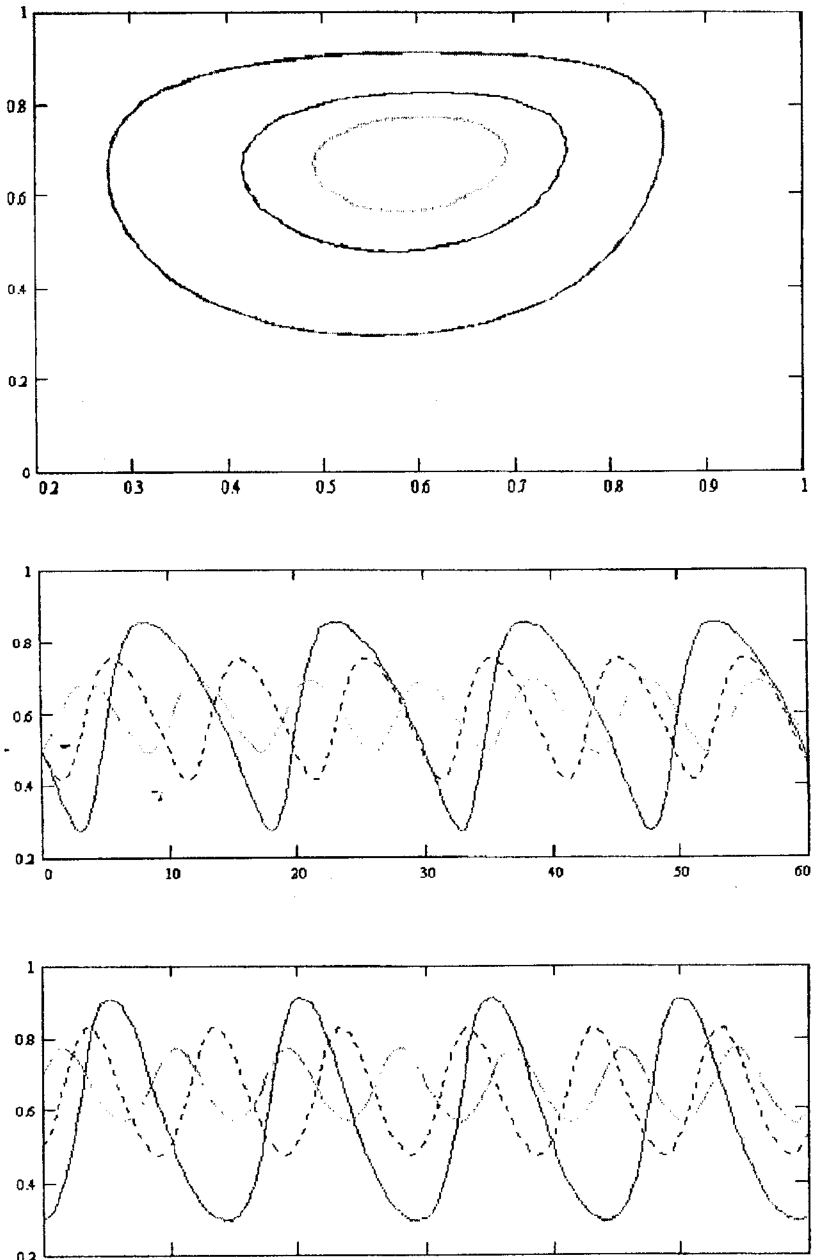

Figure 9: Re=10, Newtonian fluid after 100s, T=2s Initially placed in vertical line

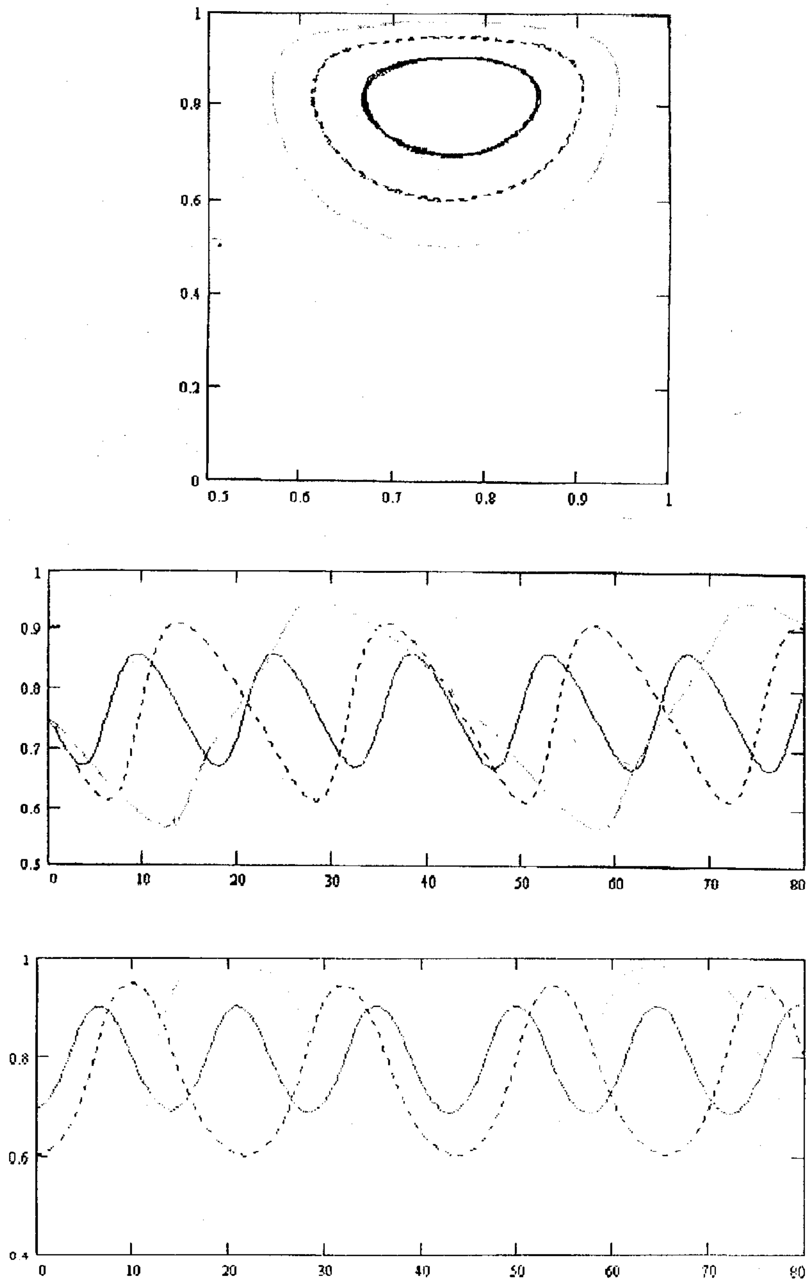

Figure 10. Re=10, Newtonian fluid after 80s, T=2s Initially placed in vertical line

at (0.75, 0.5) and occurs at more place in the cavity. Moreover, all three particle become 'flatter' near the top wall of the cavity. This behaviour shown in figure 10 for the Newtonian fluid after 80s in simulation time. As Re increases the outer particle (top figure) moves to the top wall where it remains thereafter. Moreover, the inner particles move faster and occurs at more places in the cavity. Also it can be seen that the particle paths are 'tightly bound' due to advection term dominates to flow. The middle and lower figures show the traces obtained of the periodic motion of the particles by considering the r and z with time.

6. CONCLUSION

In the 3D numerical simulation indicates that the investigation of mixing behavior and particle paths of viscous and viscoelastic fluids with constant or variable viscosity by using a cavity flow domain on a discretised field with an acceptable amount of error. In this paper new results for shear-dependent viscoelastic fluid flow were found. Mixing properties are sought in two cases: firstly by analysing the dispersive mixing of a 'coloured' portion of the fluid 'injected' into cavity at rest and secondly by the tracing of a number of selected fluid particles within the cavity by using discontinuous periodic wall motion. The results of viscoelastic fluid to be almost industinguishable from the viscous flow. In other word there is no much difference between the viscous and viscoelastic flow propagation in the flow domain. The flow process is very stable or low Re and as Re number increases the advection term starts dominating the flow. Furthermore, for low Reynolds number the 'coloured' band spread out horizontally in the cavity's centre region because of the relatively weak flow induced and diffusion was dominant. As the Reynolds number increases there is better fluid transportation and associated dispersive mixing. Specially in many cases the concentration intensity is seen to spread out more quickly near the left wall in case of the non-Newtonian fluid. On considering mixing properties by tracking particles paths, it was found that for low Reynolds number the particles followed 'flatter' paths nearer the top plate. Moreover, as Re increases the particle paths become more 'tightly bound' in the flow for both the cylinder and concentric cylinder cases. In addition, the outer particle path was found to stop against the top wall at Re=20 for concentric cylinder case.

Acknowledgment

This is the part of the study which has been carried out at he University of Glamorgan and the author would like to thank Dr. R.W. Williams for his interest and encouragement.

REFERENCES

[1] CROCHET, M.J., DAVIES, A.R. and WALTERS, K.: Numerical Simulation of non-Newtonian Flow. Rheology Series 1, Elsevier 1984.

[2] DEMİR, H.: Mixing properties of a viscoelastic fluid; Part I, In a 2 D cavity Flow. Communications, Fac. Sci. Univ. Ankara Series A2-A3, Vol. 44 (1997) 1-16.

[3] MORGAN, K. et al.: Computer Methods in Fluids. Pentech Press, London: Plymouth 1980.

[4] MORTON, K.Y. and MAYERS D.F.: Numerical Solution of Partial Differential Equations. Cambridge University Press 1994.

[5] SCRATON, R.E.: Further Numerical Methods In Basıc. Edward Arnold 1987.

[6] SMITH, G.D.: Numerical Solution of Partial Differential Equations: Finite Difference Methods. Second Edition. Clarendon Press Oxford 1978.

COMMUNICATIONS

DE LA FACULTE DES SCIENCES
DE L'UNIVERSITE D'ANKARA

FACULTY OF SCIENCES
UNIVERSITY OF ANKARA

Séries A2-A3: Physics, Engineering Physics and Astronomy

INSTRUCTIONS TO CONTRIBUTORS

Communications accepts original research articles and letters to the Editor in various fields of research in physics, engineering physics and astronomy. Contribution is open to researchers of all nationalities.

Manuscripts should be written in English. Each paper should be preceded by an abstract in English. They must be type-written using a font style and size which is quite legible, double-spaced throughout with ample margins and single-sided on white A4 standard paper. Manuscripts submitted for publication should contain one original and two complete copies; single or incomplete texts will not be accepted and will not be returned.

After the manuscript has been accepted for publication, i.e., after referee-recommended revisions are complete, the author will not be permitted to make any new additions to the manuscript.

Attention: before publication the galley proof is always sent to the author for corrections. Thus, it is solely the author's responsibility for any typographical mistakes which occur in their article as it appears in the journal. Only those mistakes/omissions which occur due to some negligence on our part during the final printing will be reprinted in a Corrections section of a later issue. However, this does not include those errors left unnoticed by the author on the galley proofs.

1. Title Page

The title should be short in length but informative. Each title page should contain:

(i) Name of the paper, (ii) Complete name(s) of the author(s), (iii) Name and address of the university, laboratory or institute at which the reseacrh has been carried out.

2. Abstract

Each paper should always be preceded by an abstract. The abstract should be short and self-contained and all essential points of the paper should be mentioned.

3. Sections and Subsections

Principle sections such as introduction or formulation of the problem should be numbered consecutively (1. Introduction, 2. Formulation of the problem, ..., etc.) Subsections should be numbered 1.1, 1.2, ..., etc.

4. References

References including comments must be numbered consecutively in order of first appearance in the text. The reference number should be put in brackets [1] where referred to in the text. References should be listed at the end of the manuscript in the numbered order in which they appear in the text. The method of citation should be as follows:

Articles in Periodicals: (i) Surname(s) of the author(s) with their initial(s), (ii) Title of the periodical abbreviated according to the "Physics Abstract list of journals", (iii) Volume number, (iv) Year of publication, (v) Page number.

Example: M. Chen and P.M. Zerwas, Phys. Rev. D 12 (1975) 187.

Books; (i) Surname(s) of the author(s) with their initial(s), (ii) Title of the book, (iii) Name of the editor (if any), (iv) Volume number, (v) Place and year of publication and name of the publisher, (vi) Page number.

Example: A. Arima, Progress in particle and nuclear physics, ed. D. Wilkinson, vol. 1 (Pergamon, New York, 1978) p. 41.

Theses: (i) Surname and initials of the author, (ii) Type of degree (Ph.D., M.Sc.), (iii) Name and address of institute where the work has been carried out, (iv) Year.

Example: H. Parker, Ph D Thesis, Department of Physics, Univ. of California, Davis, CA 95616, USA, 1990.

5. Footnotes

Footnotes should be avoided if possible, but when necessary, should be short and never contain any important part of the work and should be numbered consecutively by superscripts.

6. Tables and Figures

All illustrations not including tables (photographs and other films, drawings, graphs, etc) must be labeled as "Figure".

The proper position of each table and figure must be clearly indicated in the paper.

All tables and figures must have a number (Table 1, Figure 1) and a caption or legend. If there is only one table or figure simply label it "Table" or "Figure".

All tables and figures must be numbered consecutively throughout the paper.

All captions and legends must also be double-space typed on a separate sheet and labeled according to which table or figure they belong.

Dimensions of tables and figures must not exceed 13x16 cm.

Tables must be clearly typed, each on a separate sheet, and double-spaced. Dimensions including caption, title, column heads, and footnotes must not exceed 13x16 cm. Tables may be continued onto another sheet if necessary but dimensions still apply.

Figures must be originals and drawn clearly in Indian ink on white paper or printed on smooth tracing/drawing paper. Reduced photocopies are not acceptable. Photographs must be clear, black and white, and printed on glossy paper.

7. Appendices

All appendices must be typed on separate sheets and should be numbered consecutively with capital Roman numerals.

8. Computer Disk:

If you are able to initially prepare your manuscript in a MS Word Programme (Macintosh or PC) file including the figures translated into the picture environment of Encapsulated PostScript format (EPS), we advise that you do so. Then, only if and after your manuscript is accepted for publication, we will ask you to submit a revised disk copy of your manuscript which will enable us to more efficiently and accurately prepare proofs. (This is not a requirement but is highly encouraged.)

9. Address:

Texts should be sent to the following address:
Prof.Dr. Öner ÇAKAR - Editor, Communications
Ankara Üniversitesi, Fen Fakültesi
06100, Beşevler-ANKARA

COMMUNICATIONS

DE LA FACULTE DES SCIENCES
DE L'UNIVERSITE D'ANKARA

FACULTY OF SCIENCES
UNIVERSITY OF ANKARA

Volume: 44 **Number: 1-2** **Year: 1997**

CONTENTS